THE JOURNAL OF PHYSICAL CHEMISTRY B

Article

pubs.acs.org/JPCB

Experimental Evidence of Fermi Resonances in Isotopically Dilute Water from Ultrafast Broadband IR Spectroscopy

Luigi De Marco, Krupa Ramasesha,[†] and Andrei Tokmakoff*[,‡]

Department of Chemistry, Massachusetts Institute of Technology, 77 Massachusetts Avenue, Cambridge, Massachusetts 02139, United States

ABSTRACT: The vibrational dynamics of liquid water, which result from a complex interplay between internal molecular vibrations and the fluctuating hydrogen bond network, are fundamental to many physicochemical and biological processes. Using a new ultrafast broadband mid-infrared light source with over 2000 cm^{-1} of bandwidth, we performed ultrafast time-resolved infrared spectroscopy to study the vibrational couplings and relaxation dynamics of the stretching and bending vibrations of the mixed isotopologue, HOD, in D_2O. Analysis of cross-peaks and induced absorptions in the two-dimensional infrared spectrum and transient absorption spectrum shows that the hydroxyl stretch of HOD is coupled to the HOD bending mode via Fermi resonance, with a 70° angle between their transition dipole moments. We see that HOD is also anharmonically coupled to the D_2O solvent modes. From transient absorption spectra, we conclude that vibrational relaxation occurs through a number of paths. The strongly hydrogen-bonded OH oscillators have the highest propensity to relax through the bending mode, while the weakly hydrogen bonded oscillators relax through other modes.

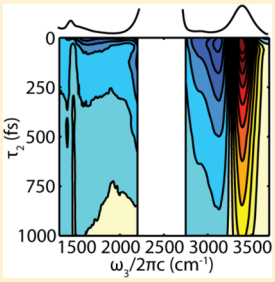

I. INTRODUCTION

The vibrational dynamics of water molecules in the liquid phase are of fundamental importance to many chemical and biological processes, such as the active participation in aqueous chemical reactions or the stabilization of reactive products[1] and the molecular transport of charges and energy.[2] These ultrafast dynamics are particularly complex due to the strong dependence of intramolecular stretching and bending vibrations on the intermolecular structure of the hydrogen bond network. At this time, few experimental methods have been able to directly describe the interaction between multiple vibrational degrees of freedom as a result of the wide-range of vibrational frequencies involved and the femtosecond time scale of their motions.[3,4] With the development of a new femtosecond broadband infrared (BBIR) laser source, which has sub-70 fs time resolution and spectral bandwidth throughout the mid-IR,[5−8] there now exist new possibilities for studying these interactions.

In this work, we use a BBIR laser source to investigate the two high-frequency vibrations, the hydroxyl stretch and water bend, the coupling between these two modes, and the relaxation of these modes upon excitation of the hydroxyl stretch. To observe the effect of local excitation and to minimize resonance energy transfer effects, we study vibrational correlations between the stretching motion and bending motion of isotopically dilute HOD in D_2O. Using femtosecond BBIR transient absorption (TA) and two-dimensional infrared (2DIR) spectroscopy, we can monitor correlations between the stretch and the bend directly by looking at cross-peaks between the two vibrations.

The dependence of the internal vibrational frequencies on hydrogen-bonding configuration plays a particularly important role in these dynamics. It is a well-accepted fact that the OH stretching frequency of dilute HOD in D_2O is highly sensitive to its local environment, which is determined primarily by the hydroxyl's hydrogen-bond configuration.[9−11] Hydroxyl oscillators that are in strongly hydrogen-bonded configurations tend to absorb at lower frequencies, while weakly or non-hydrogen-bonded oscillators tend to absorb at higher frequencies. An opposite trend is observed for the HOD bend; the HOD bending mode blue-shifts upon forming strong hydrogen bonds with the hydroxyl and deuteroxyl oscillators.[12] Upon the formation of a strong hydrogen bond, the OH stretch is red-shifted (while the HOD bend is slightly blue-shifted) and brought closer into resonance with the overtone of the HOD bend. This is expected to have a profound impact on the vibrational coupling between these modes.

Given its utility in these studies, it is no surprise that the vibrational dynamics of isotopically dilute water have been studied extensively using a variety of nonlinear time-resolved IR techniques[13−26] as well as a plethora of computational methods.[27−31] From this vast body of work, a number of pathways for the relaxation of the hydroxyl stretching vibration have been proposed. For example, based on mixed IR-Raman spectroscopy, Deàk et al. concluded that relaxation occurs via significant intermolecular stretch-to-bend transfer, resulting ultimately in the generation of DOD bend excitation.[20] This is in contrast with Nienhuys et al., who used two-color pump−probe to determine that the bend does not participate significantly in the OH stretch relaxation but rather that the hydrogen bonds are the dominant accepting mode.[25] Similarly, the relative importance of intramolecular versus intermolecular vibrational relaxation remains unclear.[28,32]

Special Issue: Michael D. Fayer Festschrift

Received: April 8, 2013
Revised: April 30, 2013

   dx.doi.org/10.1021/jp4034613 | J. Phys. Chem. B XXXX, XXX, XXX−XXX

We seek to precisely determine the nature of the coupling between the OH stretch and the HOD bend and how it affects the relaxation out of the OH stretching mode. To do this, we use both TA and 2DIR spectroscopy in which the spectral bandwidth of the probe pulse is over 2000 cm^{-1}; this allows us to monitor the entire vibrational spectrum of HOD upon excitation of the OH stretch. If the stretch−bend coupling is the dominant relaxation mechanism of the OH stretch, then it stands to reason that this will be reflected in the time evolution of the cross-peaks in the nonlinear spectra. Our findings indicate that the OH stretch and HOD bend fundamentals are coupled via a Fermi resonance, as are the overtone states, and that relaxation occurs through a mixture of paths that involve both the HOD bend and intermolecular interactions.

II. EXPERIMENTAL SECTION

In this work, we use ultrafast pulses of BBIR light as a probe in TA spectroscopy and 2DIR spectroscopy. The basic principles of these experiments have been described in great detail elsewhere,[33−35] so only a brief overview is given here. The excitation or pump pulses in these experiments are 45 fs pulses centered at 3400 cm^{-1} with 330 cm^{-1} of bandwidth, which are generated using the OPA design of Fecko et al.[36] The probe pulses are BBIR pulses with over 2000 cm^{-1} of spectral bandwidth, which easily covers the OH stretch and HOD bending modes, which peak at 3405 and 1460 cm^{-1}, respectively.

The BBIR is generated via the scheme of Petersen and Tokmakoff,[5] which extends generation methods previously used in the terahertz regime[37,38] to the mid-IR. In brief, 25 fs pulses of 800 nm light are type-I frequency-doubled in BBO to generate 400 nm light. A dual-frequency waveplate is used to rotate the polarization of the residual 800 nm light onto the polarization of the 400 nm light, and temporal-walkoff in the waveplate is precompensated for using a birefringent crystal. The 800 and 400 nm pulses are then summed to generate 267 nm in a second type-I process; the resulting beam consists of the residual 800 and 400 nm and the orthogonally polarized 267 nm third harmonic copropagating in time and space. The pulses are then focused using a double-coated 10 cm radius dielectric mirror into a gentle stream of dry air. The large electric field of the pulses results in the generation of a plasma at the focal point from which the BBIR is radiated. The resulting BBIR is collimated at a diameter of ∼15 mm. Residual visible light is filtered off with a 400 μm thick, high-resistivity silicon wafer that also serves as a point of overlap for a visible HeNe tracer beam. The polarization of the broadband, measured just before the sample, is found to be linearly polarized at an angle of +20° from vertical. The BBIR is peaked at ∼2500 cm^{-1} and the spectral bandwidth is limited by the detector and efficiency of the grating; practically, we can currently detect frequencies between 4000 and 1350 cm^{-1}. Cross-correlation of the BBIR with an IR pulse of a known 45 fs length results in a Gaussian interferogram with a standard deviation of ∼70 fs, resulting in an estimated BBIR pulse length of ∼50 fs.

In TA spectroscopy, an IR pump pulse vibrationally excites the sample, and the transient absorption of the sample is measured with a BBIR probe pulse after an experimentally controlled time delay, τ_2. The TA signal is observed by dispersing the transmitted probe pulse in a monochromator onto a 64 pixel mercury−cadmium−telluride CCD array, which can, for any particular grating angle, measure ∼1.5 μm of spectral bandwidth. It is necessary to collect data at multiple grating positions and stitch the spectra together to acquire a full BBIR spectrum. The final spectrum is plotted as the change in absorbance. The TA spectra were collected for 66 unequally spaced τ_2 points between −1 and 6 ps with detection frequencies ω_3 = 1350−2200 cm^{-1} and ω_3 = 2750−3700 cm^{-1}. The ω_3 region in between is not collected due to the high absorption of the OD stretch of the solvent.

Two-dimensional IR measurements were performed in the pump−probe geometry.[39] This experiment is similar to TA spectroscopy except that the pump frequency is measured interferometrically for each waiting time. Using a Mach−Zehnder interferometer, the pump pulse is split and recombined as two collinear pulses, which are separated in time by an experimentally controlled time delay τ_1. The 2DIR differential absorption signal is Fourier-transformed in τ_1, which gives the change in absorbance as a function of two frequency variables ω_1 and ω_3, for a fixed value of τ_2. Projection of the 2DIR surface onto ω_3 is equal to the TA spectrum at the same waiting time. The 2DIR spectrum is collected in the frequency regions of ω_3 = 1350−1600 cm^{-1} and ω_3 = 2750−3700 cm^{-1} and was collected only for τ_2 = 100 fs for this study. All TA and 2DIR spectra reported in this paper are taken with parallel polarization (ZZZZ) of both the pump and probe pulses unless otherwise stated.

Isotopic water solutions were prepared by mixing H_2O, purified by reverse osmosis (to a resistance of 18 MΩ), with D_2O (>99.96%D, Cambridge Isotope Laboratories) in a ratio of 1:99. This results in a ∼2% mole fraction (1.67 M) solution of HOD in D_2O, with a negligible amount of H_2O present. Samples were held between 1 mm thick CaF_2 windows separated by a 50 μm Teflon spacer. To avoid spectral distortions caused by the nonresonant electronic response of the CaF_2 windows, we studied spectral features only for waiting times equal to or longer than 100 fs.

III. RESULTS AND DISCUSSION

a. Linear Spectra. The linear IR absorption spectra for dilute HOD in D_2O and pure D_2O are shown in Figure 1a. The D_2O spectrum shows three principle features: a broad peak at 2505 cm^{-1} corresponding to the OD stretching vibrations, a narrower peak at 1210 cm^{-1} corresponding to the DOD bending mode, and a broad low-intensity feature at 1555 cm^{-1} that has been attributed to a combination band of the bend and the ∼400 cm^{-1} librational mode.[40]

The spectrum of HOD in D_2O shows additional features corresponding to the OH stretch, centered at 3405 cm^{-1}, and the HOD bend at 1460 cm^{-1}; the OD stretch of the HOD molecule is masked by the D_2O absorption. In addition to these intense features, a weak peak is observed at 2950 cm^{-1} (Figure 1b), which has been assigned to the overtone of the HOD bend.[19,41,42] Correction for the background yields a center frequency of 2925 cm^{-1}. Given that overtone transitions of vibrations are weak compared with the fundamental transitions, it is surprising that the HOD bend overtone would be visible in the absorption spectrum at all. This suggests that the oscillator strength of the bend overtone is increased by mixing with other modes, namely, the OH stretch, OD stretch, or solvating D_2O molecules. On the basis of the common observation of Fermi resonance enhancements in IR spectra for methyl and methylene[43,44] and other hydride stretching vibrations[45] that have near 2:1 frequency ratios between stretch and bend, it is likely that this interaction exists for the HOD molecule as well.

dx.doi.org/10.1021/jp4034613 | J. Phys. Chem. B XXXX, XXX, XXX−XXX

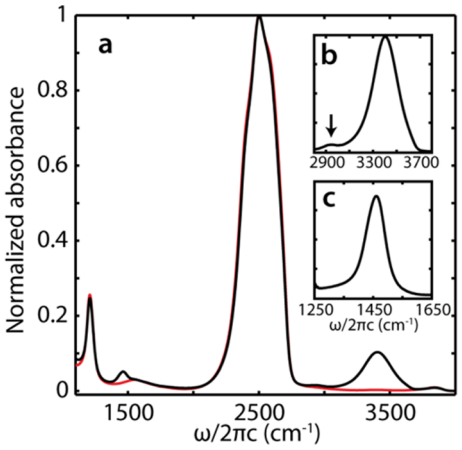

Figure 1. (a) Normalized linear infrared absorption spectra of 2% HOD in D_2O (black) and neat D_2O (red) taken in a 50 μm path length CaF_2 liquid cell. (b) Absorption spectrum of the stretching region for 2% HOD in D_2O, corrected for the D_2O absorption background. The arrow at 2950 cm^{-1} indicates the position of the overtone of the HOD bend, the intensity of which is expected to arise from Fermi resonances between the HOD bend and the OH and OD stretches. (c) Absorption spectrum of the bending region for 2% HOD in D_2O, corrected for the D_2O absorption background.

Interestingly, while Fermi resonance can exist between the HOD bend and either OH or OD vibrations, the stretch oscillators that mix with the bend most strongly must have different hydrogen-bonding interactions to optimize the resonance condition. The general trends for shifts in the frequency of stretch, bend, and their overtones and combination bands as a function of hydrogen bonding interactions are summarized schematically in Figure 2.

As a hydroxyl oscillator engages in an increasingly strong hydrogen bond, the OH stretch frequency red-shifts and comes into better resonance with the HOD bend overtone at 2925 cm^{-1}. OD stretch oscillators are in better resonance with the HOD bend overtone when they are weakly hydrogen-bonded or blue-shifted. Because the bend frequency will, to a large extent, be determined by both of these hydrogen bonds, simple correlations between the hydroxyl hydrogen bond and HOD bend frequency are not expected. Based solely on its frequency shift from the stretching vibrations it is equally likely that both the OH (3405 cm^{-1}) and OD stretching vibrations (2505 cm^{-1}) couple to the HOD bend overtone. We note that this is very different from the HOD Fermi resonance in the gas phase, where the bend overtone is in almost perfect resonance with the OD stretch but ~1000 cm^{-1} off-resonance with the OH stretch. Therefore, while the cubic force constant between the OH stretch and the HOD bend overtone in the gas phase has been calculated to be 171 cm^{-1}, the effect of this coupling is expected to be small due to the large splitting between the two states.[46]

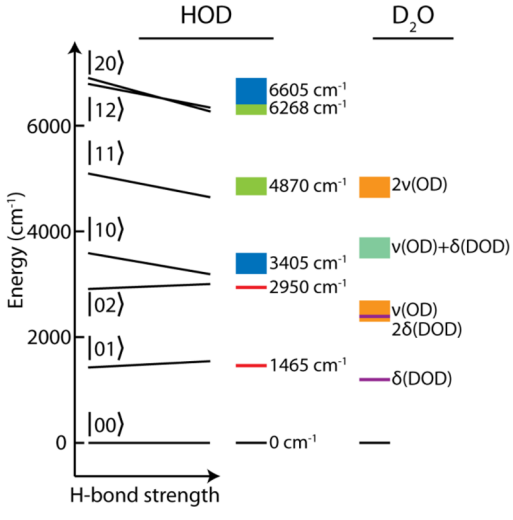

Figure 2. (left) Schematic energy level diagram for HOD stretch and bend modes that illustrate shifts as a function of hydrogen bond strength representative of the liquid. States are labeled as $|n_s n_b\rangle$ where n_s is the number of quanta in OH stretch and n_b is the number of quanta in HOD bend. (right) Colored bands show the corresponding line widths for the HOD states and for liquid D_2O. Center frequencies and line widths for states are based on observations in the linear and nonlinear IR spectra, except for the $|11\rangle$ state, which is just plotted as the sum of the $|01\rangle$ and $|10\rangle$ states.

b. Short Time Nonlinear Spectra. TA and 2DIR spectra allow us to probe the spectrum of states that are typically not accessible in the linear spectra, including induced absorptions and cross-peaks that reflect coupling between various states. The TA spectrum upon excitation of the OH stretch at 3400 cm^{-1} for τ_2 = 100 fs and τ_2 = 6 ps and the 2DIR spectrum for τ_2 = 100 fs of HOD in D_2O are shown in Figures 3a and 4,

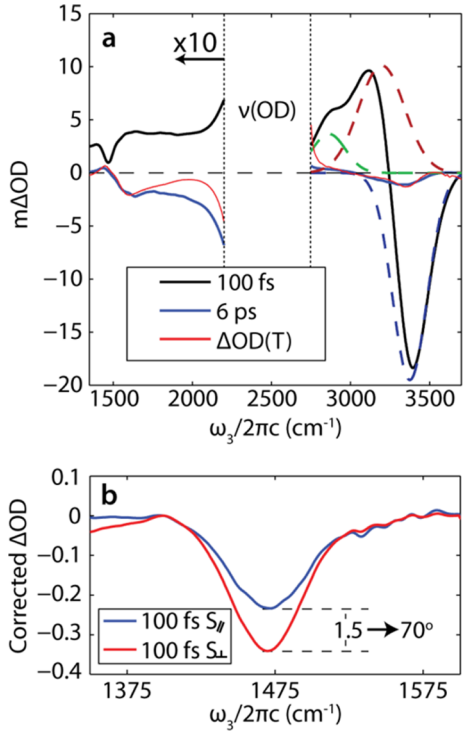

Figure 3. (a) Slices of the TA spectrum taken at τ_2 = 100 fs (solid black curve) and τ_2 = 6 ps (solid blue curve). Features below 2200 cm^{-1} are scaled up by a factor of 10. The fundamental bleach and $|n_s n_b\rangle$ = $|10\rangle \rightarrow |20\rangle$ and $|n_s n_b\rangle$ = $|10\rangle \rightarrow |12\rangle$ induced absorptions of the 100 fs spectrum are fit to Gaussians shown as dashed lines colored blue, red, and green, respectively. At early times, a clear bleach of the HOD bend fundamental is observed at 1470 cm^{-1}. At 6 ps, the TA spectrum resembles the thermal difference linear spectrum upon heating the sample from 20 to 23 °C (solid red curve). (b) TA spectra of the bend bleach at τ_2 = 100 fs for parallel and perpendicular probe polarization after baseline correction.

dx.doi.org/10.1021/jp4034613 | J. Phys. Chem. B XXXX, XXX, XXX−XXX

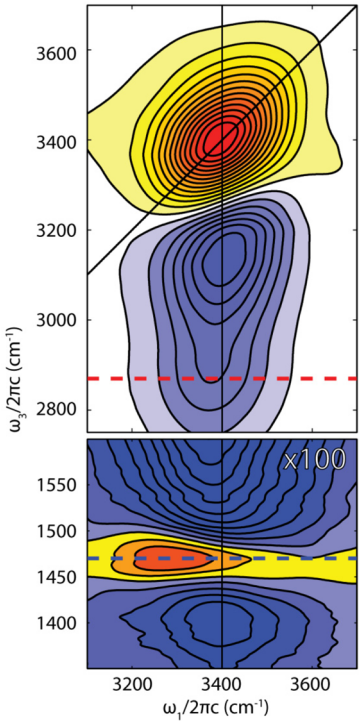

Figure 4. Broadband 2DIR spectrum of 2% HOD in D_2O. Red contours are negative (bleach) and blue contours are positive (induced absorption) The low-frequency panel has been plotted on a 100× scale relative to the high frequencies. The feature at (ω_1, ω_3) = (3375 cm^{-1}, 2870 cm^{-1}) is due to a Fermi resonance between the $|20\rangle$ and $|12\rangle$ states of HOD. The cross-peak to the fundamental of the bend is peaked at (ω_1, ω_3) = (3290 cm^{-1}, 1470 cm^{-1}), with a tail to the high frequency side in ω_1. The red and blue dashed lines correspond to slices shown in Figure 5, while the vertical black line illustrates the center frequency of the pump pulse.

respectively. Even at the earliest waiting times, bleaches and induced absorption features appear in all spectral regions in the TA and 2DIR spectra. These are located not only at transition frequencies observed in the linear spectrum, which are clearly due to stretching and bending motions, but also at frequencies whose assignments are not clear and may originate in the D_2O solvent.

At frequencies above 2750 cm^{-1}, in the OH stretching region, the 100 fs TA spectrum shows a prominent bleach as well as two distinct induced absorption peaks. The bleach at 3400 cm^{-1} is due to the pump-induced depopulation of the OH stretch ground state as well as stimulated emission induced by the probe from the first excited state of the OH stretch. The induced absorption centered at 3120 cm^{-1} is the transition from the first to second excited state of the OH stretch. This feature is red-shifted from the bleach of the fundamental transition due to the anharmonicity of the nuclear potential of the OH bond.

The bleach and induced absorption features overlap, so it is not possible to determine the anharmonicity and center frequencies directly. To do so, the three features are fitted to Gaussians, shown in Figure 3a. The anharmonicity of the OH stretch is taken to be the difference of the center frequency of the Gaussians. This procedure yields a bleach centered at $\langle\omega_{10}\rangle$ = 3375 cm^{-1} and an induced absorption centered at $\langle\omega_{21}\rangle$ = 3200 cm^{-1}, which leads to an anharmonic shift of 175 cm^{-1}. Because fitting data to the sum of overlapping Gaussians of opposite sign is typically not robust, we calculated constrained fits where the anharmonicity was held constant and the width of the fundamental bleach was forced to match the linear spectrum. Using the sum of the squares of the residuals to quantify the goodness of the fit, anharmonicities of 190 ± 20 cm^{-1} gave a reasonable fit. While this value is consistent with the near IR spectrum[47] and in reasonable agreement with cluster based DFT calculations,[48] it is significantly lower than the 250 cm^{-1} value that was reported previously and used to argue that the O−H potential is predissociative with two quanta of excitation.[49,50]

A second induced absorption peak appears as a shoulder on the excited-state absorption of the hydroxyl stretch and is centered at 2860 cm^{-1}, as determined from the Gaussian fit. Given that this feature is not observed in the linear spectrum and is at the energy of the HOD bend overtone, we are led to conclude that it results from a $|n_s n_b\rangle = |10\rangle \rightarrow |12\rangle$ transition, which has significant intensity due to a stretch−bend Fermi resonance. Here and in the following the states of the system are labeled $|n_s n_b\rangle$, where n_s refers to the number of quanta in the OH stretching mode and n_b is the number of quanta in the HOD bending mode. From picosecond TA experiments it was concluded that this feature arises due to energy transfer from the OH stretch to the HOD bend overtone;[51] however, the femtosecond time resolution in this experiment shows there is an immediate bleach indicating anharmonic coupling. Unlike the lower energy $|10\rangle$ and $|02\rangle$ states, the large anharmonic shift of the stretch relative to the bend results in the stretch overtone $|20\rangle$ (~6575 cm^{-1}) being in near-resonance with the $|12\rangle$ state, and fluctuations in hydrogen-bond strength likely cause the two states to cross in energy. The intersection of these states is illustrated in Figure 2. Comparison of the $|10\rangle \rightarrow |12\rangle$ and $|00\rangle \rightarrow |02\rangle$ transition frequencies shows that OH stretch excitation leads to a bend overtone red shift of ~90 cm^{-1}. In the idealized case of harmonic oscillators coupled by an exact 2:1 Fermi resonance, the energy shift of an overtone that results from exciting one quantum of the coupled mode is twice the strength of coupling, $\Delta = -2X_{122}$, where the Fermi resonance coupling potential is $V_{FR} = X_{122}(a_1 a_2^+ a_2^+ + a_1^+ a_2 a_2)$. The resulting 45 cm^{-1} is an upper bound on X_{122} but neglects any other off-diagonal terms. In the gas phase, this shift is only 16 cm^{-1} despite X_{122} being 60 cm^{-1}.[46] This supports strong mixing between the $|20\rangle$ and $|12\rangle$ states in the liquid phase. This coupling is accompanied by a shifting of oscillator strength from the nominally bright transition ($|n_s n_b\rangle = |10\rangle \rightarrow |20\rangle$) to the dark transition ($|n_s n_b\rangle = |10\rangle \rightarrow |12\rangle$). This redistribution results in the $|10\rangle \rightarrow |20\rangle$ induced absorption being only ~70% the intensity of the $|00\rangle \rightarrow |10\rangle$ bleach, with the other ~30% being in the $|10\rangle \rightarrow |12\rangle$ induced absorption.

The additional resolution of the pumping frequency in 2DIR provides greater insight into the Fermi resonance between the $|20\rangle$ and $|12\rangle$ states. In Figure 4, the bleach of the $|00\rangle \rightarrow |10\rangle$ fundamental transition is peaked at (ω_1, ω_3) = (3400 cm^{-1}, 3400 cm^{-1}) and appears elongated along the diagonal due to inhomogeneous broadening, while the induced absorption of the $|10\rangle \rightarrow |20\rangle$ transition is centered at (ω_1, ω_3) = (3400 cm^{-1}, 3140 cm^{-1}). The spectrum in this region is in good agreement with previous work.[23,52−54] As in the TA spectrum, the $|10\rangle \rightarrow |12\rangle$ induced absorption (ω_1, ω_3) = (3375 cm^{-1}, 2870 cm^{-1}) appears just below the $|10\rangle \rightarrow |20\rangle$ transition in ω_3 but peaked at a somewhat lower excitation frequency than the bleach. This is most clearly illustrated in Figure 5 by the comparison of a slice of the 2DIR spectrum taken at ω_3 = 2870 cm^{-1} (red) with

dx.doi.org/10.1021/jp4034613 | J. Phys. Chem. B XXXX, XXX, XXX−XXX

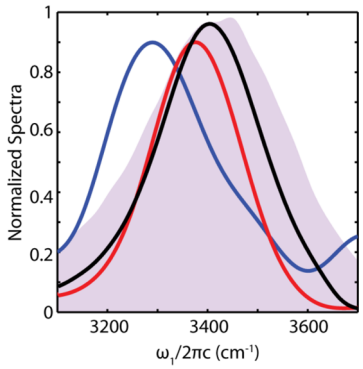

Figure 5. Normalized slices of the 2DIR spectrum along ω_1. Slice of the $|n_s n_b\rangle = |10\rangle \rightarrow |12\rangle$ induced absorption at ω_3 = 2870 cm^{-1} (red curve) peaks at ω_1 = 3375 cm^{-1} and the bend cross-peak bleach at ω_3 = 1470 cm^{-1} (blue curve, here positive) peaks at ω_1 = 3290 cm^{-1}. The black curve is the linear absorption spectrum of the sample, peaked at 3405 cm^{-1}, and the pink background shows the spectrum of the pump pulse, peaked at 3410 cm^{-1} with a 330 cm^{-1} bandwidth fwhm.

the linear absorption spectrum (black) and the spectrum of the pump pulse (pink background). While the ∼30 cm^{-1} red shift of the $|10\rangle \rightarrow |12\rangle$ transition in ω_1 is small compared with the OH line width, it does indicate that OH oscillators in stronger than average hydrogen-bond configurations have enhanced Fermi resonance between the $|20\rangle$ and $|12\rangle$ states.

At frequencies below 2200 cm^{-1}, the TA and 2DIR spectra for τ_2 = 100 fs show clear evidence of stretch−bend vibrational coupling. Both spectra show a broad induced absorption, stretching along ω_3, upon which we see a narrow bleach of the HOD bend, centered at ω_3 = 1470 cm^{-1}. The bleach arises from pump-induced depopulation of the vibrational ground state, which is consistent with the observations from picosecond IR-pump/Raman-probe experiments.[19,20] The immediate observation of the bleach with our <70 fs time resolution implies that the OH stretch and HOD bend are strongly coupled. In the weak coupling limit, the cross-peak would grow in with waiting time as population relaxes from the OH stretching mode to the lower lying bending mode. Instead, a cross-peak is observed immediately upon excitation, implying that the "OH stretching" vibration is mixed with bend degrees of freedom. This strong interaction is somewhat surprising given that stretch and bend fundamentals are split by ∼2000 cm^{-1} but is consistent with a Fermi resonance between the HOD stretch and bend states. The Fermi resonance between $|10\rangle$ and $|02\rangle$ shifts the $|10\rangle$ state to higher frequency, which results in the $|00\rangle \rightarrow |01\rangle$ and the $|10\rangle \rightarrow |11\rangle$ transitions having different frequencies. This effect should result in a cross-peak in the transient spectra between the red-shifted OH oscillators and the bend. The blue shift of this bleach relative to the linear spectrum suggests that the strongly hydrogen-bonded oscillators are most strongly coupled to the OH stretch. The TA and 2DIR spectra clearly show the stretch−bend cross-peak overlapped with a broad induced absorption that extends more than 1000 cm^{-1} from the low-frequency edge of the OD stretch absorption to frequencies well below the bending vibration.

Polarization-dependent TA measurements of the bend bleach at τ_2 = 100 fs are shown in Figure 3b. After using a linear correction for the background, we observe that the depth of the bleach increases by 150% going from parallel to perpendicular polarized pumping. This ratio of bleach intensities corresponds to a projection angle of ∼70° between the transition dipole moment of the OH stretch and the HOD bend.[55] This angle is considerably larger than the half angle between the bonds, which is expected from the fact that the OH transition dipole moment is observed to be offset from the hydroxyl bond by ∼20° in the gas phase[56] and from the small oscillation amplitude of the deuterium compared with hydrogen in the bending mode.

The 2DIR spectrum provides insight into the nature of the coupling between the stretch and the bend. The cross-peak is asymmetric, with its peak at (ω_1, ω_3) = (3290 cm^{-1}, 1470 cm^{-1}) and a tail that extends to high frequency in ω_1. Overall, the peak is weakly anticorrelated with the OH stretch, with the cross-peak absorbing at ω_3 = 1455 cm^{-1} for blue stretch excitation but at ω_3 = 1475 cm^{-1} for red stretch excitation. This anticorrelation reflects the trend of the bending mode blue-shifting upon the OH forming stronger hydrogen bonds, as is evident from the temperature dependence of the linear spectrum.[12] The fact that the cross-peak is not centered at the center frequency of the pump or linear spectrum suggests that there is a frequency-dependent coupling between the stretch and the bend. The blue line in Figure 5 shows a slice of the 2DIR spectrum taken at ω_3 = 1470 cm^{-1}, which shows that the cross-peak is peaked 115 cm^{-1} to the red of both the linear absorption (black line) and the pump spectrum (pink background). The fact that the cross-peak is shifted to the red side of the OH stretch shows that the strongly hydrogen-bonded hydroxyl oscillators (i.e., the red-shifted ones) are more strongly coupled to the bend, which is consistent with OH stretch-HOD bend coupling arising from a Fermi resonance.

Typically cross-peaks in nonlinear vibrational spectra appear in doublets: a bleach corresponding to the depopulation of the vibrational ground state and an induced absorption corresponding to an excited-state transition. From the 100 fs TA spectrum in Figure 3a and the 2D spectrum in Figure 4, no induced absorption as narrow as the bleach of the bend transition is evident, making assignment of a $|n_s n_b\rangle = |10\rangle \rightarrow |11\rangle$ transition ambiguous. This would suggest that the $|n_s n_b\rangle = |10\rangle \rightarrow |11\rangle$ transition has little oscillator strength, has a frequency that is outside our detection range, or is extremely broad. Of these three possibilities, the last one is the most likely. Overall the TA spectrum between ω_3 = 1350 and 2000 cm^{-1} appears as a bleach of the bend superimposed on a broad background that gently peaks in the bend region. Fitting can be used to estimate that its maximum is near 1660 cm^{-1}; however, significant overlap with the response of the OD stretch makes it difficult to confidentially assign a frequency to this feature. A closer look at the 2D spectrum in the same region reveals that the peak excitation frequency (ω_1) for a given detection frequency (ω_3) is weakly anticorrelated, as would be expected for stretch−bend coupling. These observations suggest that the broad background possibly involves transitions to a broad distribution of stretch−bend combination bands, which have distinct bend character.

Additionally, one cannot neglect the influence of the OD stretching vibration of the HOD or the solvating D_2O molecules. The energy of the HOD $|11\rangle$ state is expected to be near or slightly lower than the sum of the stretch and bend fundamentals (4865 cm^{-1}). This is essentially in perfect resonance with the overtone of the OD stretch.[57] Coupling between the $|11\rangle$ state and the solvent ought to be extremely efficient, which contributes to the extreme broadening of the $|n_s n_b\rangle = |10\rangle \rightarrow |11\rangle$ transition.

dx.doi.org/10.1021/jp4034613 | J. Phys. Chem. B XXXX, XXX, XXX−XXX

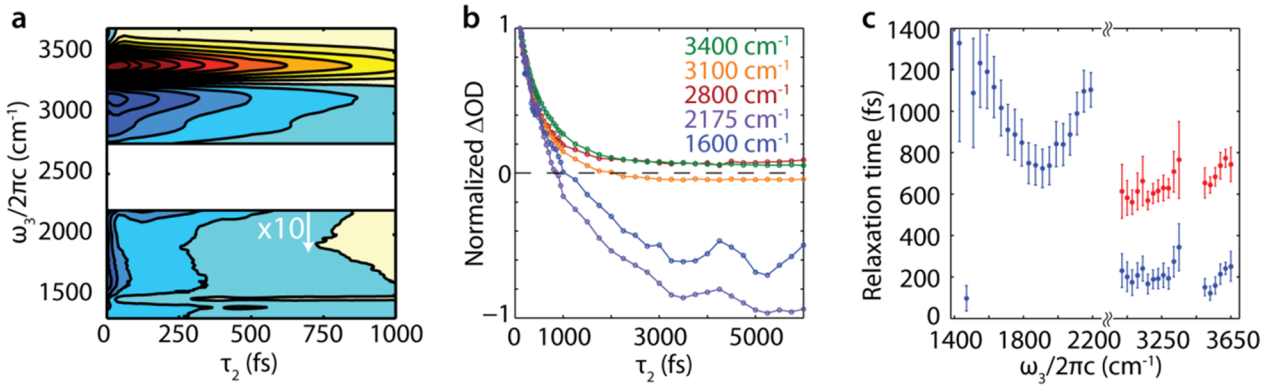

Figure 6. Spectral relaxation in transient absorption. (a) TA spectrum for 2% HOD in D_2O. (b) Decay transients at representative probe frequencies. (c) Decay time scale as a function of probe frequency. Red points show the slow time scale for the OH stretch and blue points above 2750 cm^{-1} show the fast time scale.

With the TA and 2DIR spectrum at hand, we are in a position to assign frequencies to most of the energy levels for the bend and OH stretch vibrations of HOD in Figure 2, using bands to represent broadening as a result of hydrogen bonding or vibrational coupling within the liquid. The frequencies shown are obtained from the linear or nonlinear IR spectra, except for the $|11\rangle$ state, where we report the sum of the $|01\rangle$ and $|10\rangle$ states. The correlation of the bending states with hydrogen-bond strength is somewhat exaggerated in Figure 2 because the effect of the hydrogen bonding of the HOD deuteroxyl oscillator is not taken into account. We see that the $|20\rangle$ and $|12\rangle$ states cross in energy for strong enough hydrogen bonds, while the $|10\rangle$ and $|02\rangle$ states never actually cross. Adding bands to reflect the vibrational modes of liquid D_2O emphasizes that HOD cannot be considered in isolation, as the former can strongly affect the latter. This is expected to be especially important for the D_2O stretching overtone, which is coincident with the HOD stretch−bend combination band and any intramolecular OH-OD coupling.

c. Time-Dependent Spectra. The vibrational relaxation processes that occur over 6 ps after OH stretch excitation, characterized through TA measurements, are presented in Figure 6.

Figure 6a illustrates that vibrational relaxation processes are observed at all frequencies, and representative slices taken at individual frequencies are shown in Figure 6b. Qualitatively, the relaxation time scales for probe frequencies >2800 cm^{-1} appear complete within 2 to 3 ps, whereas those below 2200 cm^{-1} are noticeably longer. From the 100 fs TA spectrum, shown in Figure 3a, relaxation processes evolve toward a TA spectrum that resembles a thermal difference spectrum at long waiting time. Figure 3a shows a comparison of the τ_2 = 6 ps TA spectrum with the 23−20 °C linear difference spectrum, showing that this close similarity, observed originally in the stretch region,[23,25] extends to all probe frequencies. The so-called "hot ground-state" (HGS) spectrum has been attributed to the local heating of the sample due to the relaxation of the excitation generated by the pump pulse,[58−60] resulting in the overall weakening in the hydrogen-bond strength in the liquid and the observed blue shift of the OH stretch.[41] Although this is a nonequilibrium system, the appearance of the HGS clearly implies that the OH stretch vibrational excitation is transferred into kinetic energy of the intermolecular motions of the liquid, leading to the average weakening of hydrogen bonds. Similarly, a blue shift of the OD stretch is evident from either side of the uncollected region in the TA spectrum: the 2750 cm^{-1} side appears as a rising edge and the 2200 cm^{-1} side shows a bleach corresponding to a blue-shifted deuteroxyl stretch. In the bending region, the HGS response is dominated by the red shift of the D_2O bend-libration combination band, which is centered at 1555 cm^{-1} in the linear spectrum, rendering the expected red shift of the HOD bend unobservable at the working concentration.

To extract frequency-dependent relaxation rates, we fit slices of the TA spectrum for constant ω_3 using robust nonlinear least-squares regression using the trust region algorithm as implemented in MATLAB. All transients are only fit for τ_2 values larger than 100 fs to avoid distortions induced by the nonresonant electronic response of the CaF_2 windows that dominates the nonlinear response in the region of pulse overlap. The relaxation of the HOD features is well-fit by either a mono- or biexponential. Time scales from these fits are reported in Figure 6c.

The decay of the OH stretch bleach has a low amplitude fast component with an average time scale of 190 ± 10 fs but is dominated by a slow time scale of 700 ± 20 fs. In previous studies the latter was attributed to the population relaxation of the OH stretch and the former to the fast intermolecular motions of the hydrogen-bonded HOD molecule.[61] As is evident from Figure 6c, the slow relaxation time scale for the bleach of the OH stretch is weakly frequency-dependent and changes linearly at a rate of ∼1.5 fs/cm^{-1}, in agreement with previous studies.[62] The frequency dependence of the relaxation time is expected to arise from a number of effects. The 2DIR spectrum shows that strongly hydrogen-bonded oscillators are more strongly coupled to the HOD bend than weakly bonded ones, which can in principle dissipate energy more efficiently via relaxation to the bend. The formation of strong hydrogen bonds also gives rise to low-frequency motions that may serve as an energy sink for the OH excitation while at the same time providing stronger coupling to the solvent. The frequency dependence is somewhat weakened as a result of rapid spectral diffusion that randomizes the OH stretch frequency on a time scale similar to the vibrational relaxation.[60] For example, in studies on polyalcohols in chloroform, where spectral diffusion is much slower, a stronger frequency dependence of the lifetime is observed.[63]

The induced absorption in the 2800 to 3150 cm^{-1} region decays on average on 200 ± 10 and 610 ± 20 fs time scales, with a weaker frequency dependence (∼0.15 fs/cm^{-1}) than the

dx.doi.org/10.1021/jp4034613 | J. Phys. Chem. B XXXX, XXX, XXX−XXX

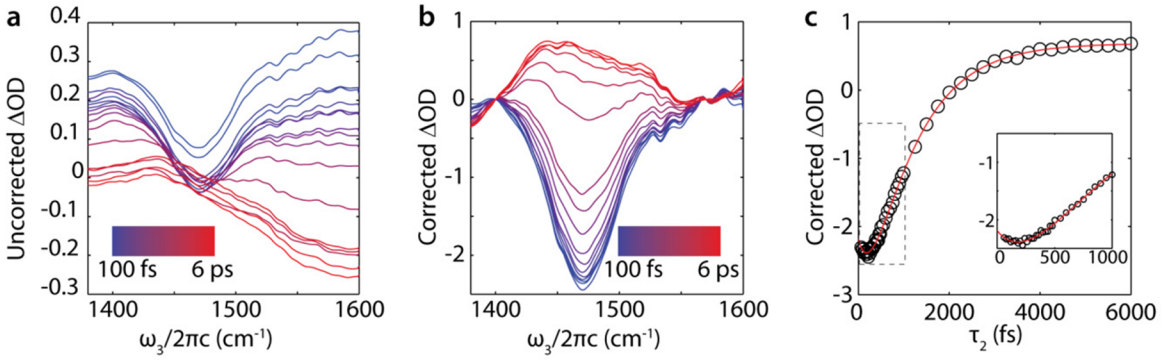

Figure 7. Relaxation of the bend. (a) Transient spectra of the bend. (b) Transient spectra corrected for the broad induced absorption by a linear background correction. (c) Decay of the bleach of the bend in the corrected spectrum. The red line shows a biexponential fit to the decay of the bleach with time components of 320 ± 40 fs and 1.01 ± 0.06 ps and amplitudes of 0.25 ± 0.05 and −0.54 ± 0.05, respectively. The inset shows the early time dynamics.

fundamental. The fact the induced absorption due to the $|n_s n_b\rangle = |10\rangle \rightarrow |12\rangle$ transition decays on the same time scale as the $|n_s n_b\rangle = |10\rangle \rightarrow |20\rangle$ transition reflects the fact that both transitions originate from the $|10\rangle$ state and decay with the lifetime of the OH stretch. The discrepancy between the 610 fs time scale for the induced absorption and the 700 fs time scale observed for the bleach can be explained by variations in long-time spectral shifts in this region.

At frequencies below 2200 cm^{-1}, the broad induced absorption that extends from the OD stretch decays with time scales varying between 750 and 1400 fs with a nonmonotonic frequency dependence. This observation is consistent with the idea that the induced absorption arises from more than one spectral feature and is not simply correlated with the relaxation of the stretch. We interpret the extended relaxation times, which are ∼1 to 2 times longer than the lifetime of the OH stretch, as indicative of complex coupling between the hydroxyl stretch and the solvating D_2O. This feature likely arises from a number of phenomena that include contributions from coupling to solvent and structural reorganization. What is clear is that the relaxation of the OH stretch is not the rate-limiting step in thermalizing the vibrational excitation, consistent with the idea that vibrational relaxation passes through an intermediate state.[25]

Because of the decay of the broad induced absorption background in this region, it is not possible to extract the relaxation time scale of the bend directly (Figure 7a); however, we can isolate it using a linear correction for the background for each τ_2 (Figure 7b). The decay of the bend bleach obtained by this procedure is fairly insensitive to the details of how the correction is applied. A biexponential fit to this data (Figure 7c) shows that the bend bleaches immediately upon pumping the stretch but then continues to grow with a 320 ± 40 fs time scale. In addition to the Fermi resonance that leads to the immediate bleach, there are additional channels for energy initially in OH stretch or bend overtone vibrations to transfer to the bend fundamental on a 320 fs time scale. The decay from the stretch to the bend can, in principle, occur with any hydroxyl stretch, but it is expected that the red-shifted oscillators will most easily transfer to the $|02\rangle$ state because these oscillators are most strongly mixed with the bend overtone. From $|02\rangle$, the energy can transfer to the solvent or into the $|01\rangle$ state. This shows that, for the strongly hydrogen-bonded oscillators, relaxation through the HOD bend is an efficient process.

The immediate response of the D_2O solvent and the HOD bend coupled to the fact that the OH stretch relaxation time is substantively longer than the 320 fs feeding of population into the bend suggest that relaxation of the OH stretch proceeds through a variety of channels that must involve both intra- and intermolecular D_2O and HOD vibrations. (We note that even in the case of intramolecular OH-OD coupling, the OD stretch of HOD is expected to be delocalized over the OD stretches of the solvent so that the distinction between "OD on HOD" and "OD on D_2O" is not possible to make.) The bend bleach recovers with a 1010 ± 60 fs time scale, which is consistent with the growth of the long-time thermal difference spectrum[25] and the relaxation of the OD stretch at ∼2200 cm^{-1}, suggesting that the bend finally relaxes into D_2O intermolecular motions. The immediate response of the OD stretch in the 2200 cm^{-1} region suggests that the OD stretches of the solvent are anharmonically coupled to the OH stretch. Its subsequent picosecond relaxation is indicative that thermalization requires structural relaxation of the liquid.

IV. CONCLUSIONS

In conclusion, we have provided evidence of Fermi resonances between the bending mode and the stretching mode of dilute HOD in D_2O. Specifically, induced absorptions in the TA and 2DIR spectra suggest the existence of a strong Fermi resonance between the $|20\rangle$ and $|12\rangle$ states of HOD. This resonance is stronger than the same cubic anharmonic interaction between the $|10\rangle$ and $|02\rangle$ states. From the TA and 2DIR spectra, it is also evident that the hydroxyl stretch is anharmonically coupled to the solvent deuteroxyl stretch and possibly other solvent modes. The strong coupling observed between the OH stretch and the other modes in the system suggests that the hydroxyl stretch is not as pure and localized as it is typically assumed to be.

From the TA spectrum, we are able to conclude that the relaxation of the OH stretch does not occur through any one mode but rather through several paths involving both the D_2O modes and the HOD bend. The strongly hydrogen-bonded OH oscillators are most strongly coupled to the $|02\rangle$ state, and relaxation is expected to occur through the bend overtone for these oscillators into either the $|01\rangle$ state or the deuteroxyl stretch. The weakly hydrogen-bonded oscillators are more likely to transfer energy directly to the solvent modes or to the bend after forming a strong hydrogen bond. Any population that penultimately ends up in bend relaxes with the same

dx.doi.org/10.1021/jp4034613 | J. Phys. Chem. B XXXX, XXX, XXX−XXX

picosecond time scale of the solvent. This picture is consistent with views previously expressed,[19,20,32] although we emphasize that the strength of couplings involved are significant enough that the character of intra- and intermolecular stretch and bend vibrations is relatively strongly mixed compared with a local mode picture of the vibrations of the system.

Finally, we emphasize that this work is but one example of numerous problems in vibrational and molecular dynamics that are opened up through the use of BBIR spectroscopy. As seen in the experiments here on a molecule as extensively studied as HOD, vibrational couplings between multiple degrees of freedom can now be immediately characterized. The ability to correlate multiple vibrational transitions throughout the mid-IR allows one to immediately characterize the intra- and intermolecular couplings of vibrations in space and in time. We look forward to a time when 2DIR spectroscopy can be performed with both dimensions spanning the entire mid-IR, including the vibrational fingerprint region.

AUTHOR INFORMATION

Corresponding Author

*E-mail: tokmakoff@uchicago.edu. Tel: (773) 834-7696.

Present Addresses

[†]Department of Chemistry, University of California, Berkeley, CA 94720.

[‡]The University of Chicago, 929 E. 57th St., Chicago, IL 60637.

Notes

The authors declare no competing financial interest.

ACKNOWLEDGMENTS

This work was funded by the U.S. Department of Energy (DE-FG02-99ER14988). L.D.M. thanks the Natural Sciences and Engineering Research Council of Canada for a fellowship.

REFERENCES

(1) Narayan, S.; Muldoon, J.; Finn, M. G.; Fokin, V. V; Kolb, H. C.; Sharpless, K. B. On Water: Unique Reactivity of Organic Compounds in Aqueous Suspension. *Agew. Chem. Int. Ed.* **2005**, *44*, 3275−3279.

(2) Agmon, N. The Grotthuss Mechanism. *Chem. Phys. Lett.* **1995**, *244*, 456−462.

(3) Lindner, J.; Vöhringer, P.; Pshenichnikov, M. S.; Cringus, D.; Wiersma, D. A.; Mostovoy, M. Vibrational Relaxation of Pure Liquid Water. *Chem. Phys. Lett.* **2006**, *421*, 563−567.

(4) Lindner, J.; Cringus, D.; Pshenichnikov, M. S.; Vöhringer, P. Anharmonic Bend−Stretch Coupling in Neat Liquid Water. *Chem. Phys.* **2007**, *341*, 326−335.

(5) Petersen, P. B.; Tokmakoff, A. Source for Ultrafast Continuum Infrared and Terahertz Radiation. *Opt. Lett.* **2010**, *35*, 1962−1964.

(6) Baiz, C. R.; Kubarych, K. J. Ultrabroadband Detection of a Mid-IR Continuum by Chirped-Pulse Upconversion. *Opt. Lett.* **2011**, *36*, 187−189.

(7) Cheng, M.; Reynolds, A.; Widgren, H.; Khalil, M. Generation of Tunable Octave-Spanning Mid-Infrared Pulses by Filamentation in Gas Media. *Opt. Lett.* **2012**, *37*, 1787−9.

(8) Calabrese, C.; Stingel, A. M.; Shen, L.; Petersen, P. B. Ultrafast Continuum Mid-Infrared Spectroscopy: Probing the Entire Vibrational Spectrum in a Single Laser Shot with Femtosecond Time Resolution. *Opt. Lett.* **2012**, *37*, 2265−2267.

(9) Fecko, C. J.; Eaves, J. D.; Loparo, J. J.; Tokmakoff, A.; Geissler, P. L. Ultrafast Hydrogen-Bond Dynamics in the Infrared Spectroscopy of Water. *Science* **2003**, *301*, 1698−1702.

(10) Eaves, J. D.; Tokmakoff, A.; Geissler, P. L. Electric Field Fluctuations Drive Vibrational Dephasing in Water. *J. Phys. Chem. A* **2005**, *109*, 9424−9436.

(11) Corcelli, S. A.; Lawrence, C. P.; Skinner, J. L. Combined Electronic Structure/Molecular Dynamics Approach for Ultrafast Infrared Spectroscopy of Dilute HOD in Liquid H_2O and D2O. *J. Chem. Phys.* **2004**, *120*, 8107−17.

(12) Falk, M. Frequencies of H-O-H, H-O-D, and D-O-D Bending Fundamentals in Liquid Water. *J. Raman. Spectr.* **1990**, *21*, 563−567.

(13) Graener, H.; Seifert, G.; Laubereau, A. New Spectroscopy of Water Using Tunable Picosecond Pulses in the Infrared. *Phys. Rev. Lett.* **1991**, *66*, 2092−2095.

(14) Yeremenko, S.; Pshenichnikov, M. S.; Wiersma, D. A. Hydrogen-Bond Dynamics in Water Explored by Heterodyne-Detected Photon Echo. *Chem. Phys. Lett.* **2003**, *369*, 107−113.

(15) Rezus, Y. L. A.; Bakker, H. J. On the Orientational Relaxation of HDO in Liquid Water. *J. Chem. Phys.* **2005**, *123*, 114502.

(16) Park, S.; Odelius, M.; Gaffney, K. J. Ultrafast Dynamics of Hydrogen Bond Exchange in Aqueous Ionic Solutions. *J. Phys. Chem. B* **2009**, *113*, 7825−7835.

(17) Ramasesha, K.; Roberts, S. T.; Nicodemus, R. A.; Mandal, A.; Tokmakoff, A. Ultrafast 2D IR Anisotropy of Water Reveals Reorientation During Hydrogen-Bond Switching. *J. Chem. Phys.* **2011**, *135*, 054509.

(18) Woutersen, S.; Emmerichs, U.; Nienhuys, H.-K.; Bakker, H. Anomalous Temperature Dependence of Vibrational Lifetimes in Water and Ice. *Phys. Rev. Lett.* **1998**, *81*, 1106−1109.

(19) Wang, Z.; Pakoulev, A.; Pang, Y.; Dlott, D. D. Vibrational Substructure in the OH Stretching Transition of Water and HOD. *J. Phys. Chem. A* **2004**, *108*, 9054−9063.

(20) Deak, J. C.; Rhea, S. T.; Iwaki, L. K.; Dlott, D. D. Vibrational Energy Relaxation and Spectral Diffusion in Water and Deuterated Water. *J. Phys. Chem. A* **2000**, *104*, 4866−4875.

(21) Stenger, J.; Madsen, D.; Hamm, P.; Nibbering, E.; Elsaesser, T. Ultrafast Vibrational Dephasing of Liquid Water. *Phys. Rev. Lett.* **2001**, *87*, 027401.

(22) Eaves, J. D.; Loparo, J. J.; Fecko, C. J.; Roberts, S. T.; Tokmakoff, A.; Geissler, P. L. Hydrogen Bonds in Liquid Water are Broken Only Fleetingly. *Proc. Natl. Acad. Sci. U.S.A.* **2005**, *102*, 13019−13022.

(23) Loparo, J. J.; Roberts, S. T.; Tokmakoff, A. Multidimensional Infrared Spectroscopy of Water. I. Vibrational Dynamics in Two-Dimensional IR Line Shapes. *J. Chem. Phys.* **2006**, *125*, 194521.

(24) Loparo, J. J.; Roberts, S. T.; Tokmakoff, A. Multidimensional Infrared Spectroscopy of Water. II. Hydrogen Bond Switching Dynamics. *J. Chem. Phys.* **2006**, *125*, 194522.

(25) Nienhuys, H.-K.; Woutersen, S.; Van Santen, R. A.; Bakker, H. J. Mechanism for Vibrational Relaxation in Water Investigated by Femtosecond Infrared Spectroscopy. *J. Chem. Phys.* **1999**, *111*, 1494.

(26) Bodis, P.; Larsen, O. F. A.; Woutersen, S. Vibrational Relaxation of the Bending Mode of HDO in Liquid D_2O. *J. Phys. Chem. A* **2005**, *109*, 5303−5306.

(27) Møller, K. B.; Rey, R.; Hynes, J. T. Hydrogen Bond Dynamics in Water and Ultrafast Infrared Spectroscopy: A Theoretical Study. *J. Phys. Chem. A* **2004**, *108*, 1275−1289.

(28) Rey, R.; Hynes, J. T. Vibrational Energy Relaxation of HOD in Liquid D_2O. *J. Chem. Phys.* **1996**, *104*, 2356.

(29) Lawrence, C. P.; Skinner, J. L. Vibrational Spectroscopy of HOD in Liquid D_2O. I. Vibrational Energy Relaxation. *J. Chem. Phys.* **2002**, *117*, 5827.

(30) Lawrence, C. P.; Skinner, J. L. Vibrational Spectroscopy of HOD in Liquid D_2O. II. Infrared Line Shapes and Vibrational Stokes Shift. *J. Chem. Phys.* **2002**, *117*, 8847.

(31) Lawrence, C. P.; Skinner, J. L. Vibrational Spectroscopy of HOD in Liquid D_2O. III. Spectral Diffusion, and Hydrogen-Bonding and Rotational Dynamics. *J. Chem. Phys.* **2003**, *118*, 264.

(32) Lawrence, C. P.; Skinner, J. L. Vibrational Spectroscopy of HOD in Liquid D_2O. VI. Intramolecular and Intermolecular Vibrational Energy Flow. *J. Chem. Phys.* **2003**, *119*, 1623.

(33) Hybl, J. D.; Albrecht, A. W.; Faeder, S. M. G.; Jonas, D. M. Two-Dimensional Electronic Spectroscopy. *Chem. Phys. Lett.* **1998**, *297*, 307−313.

(34) Hamm, P.; Lim, M.; Hochstrasser, R. M. Structure of the Amide I Band of Peptides Measured by Femtosecond Nonlinear-Infrared Spectroscopy. *J. Phys. Chem. B* **1998**, *102*, 6123−6138.
(35) Khalil, M.; Demirdöven, N.; Tokmakoff, A. Coherent 2D IR Spectroscopy: Molecular Structure and Dynamics in Solution. *J. Phys. Chem. A* **2003**, *107*, 5258−5279.
(36) Fecko, C. J.; Loparo, J. J.; Tokmakoff, A. Generation of 45 fs Pulses at 3 μm with a $KNbO_3$ Optical Parametric Amplifier. *Opt. Commun.* **2004**, *241*, 521−528.
(37) Cook, D. J.; Hochstrasser, R. M. Intense Terahertz Pulses by Four-Wave Rectification in Air. *Opt. Lett.* **2000**, *25*, 1210−1212.
(38) Kress, M.; Löffler, T.; Eden, S.; Thomson, M.; Roskos, H. G. Terahertz-Pulse Generation by Photoionization of Air with Laser Pulses Composed of Both Fundamental and Second-Harmonic Waves. *Opt. Lett.* **2004**, *29*, 1120−2.
(39) DeFlores, L. P.; Nicodemus, R. A.; Tokmakoff, A. Two-Dimensional Fourier Transform Spectroscopy in the Pump-Probe Geometry. *Opt. Lett.* **2007**, *32*, 2966−8.
(40) Maréchal, Y. Infrared Spectra of Water. I. Effect of Temperature and of H/D Isotopic Dilution. *J. Chem. Phys.* **1991**, *95*, 5565.
(41) Wyss, H. R.; Falk, M. Infrared Spectrum of HDO in Water and in NaCl Solution. *Can. J. Chem.* **1970**, *48*, 607−617.
(42) Graener, H.; Seifert, G.; Laubereau, A. New Spectroscopy of Water Using Tunable Picosecond Pulses in the Infrared. *Phys. Rev. Lett.* **1991**, *66*, 2092−2095.
(43) Snyder, R. G.; Scherer, J. R. Band Structure in the C−H Stretching Region of the Raman Spectrum of the Extended Polymethylene Chain: Influence of Fermi Resonance. *J. Chem. Phys.* **1979**, *71*, 3221.
(44) Lavalley, J. C.; Sheppard, N. Anharmonicity of CH_3 Deformation Vibrations and Fermi Resonance Between the Symmetrical CH_3 Stretching Mode and Overtones of CH_3 Deformation Vibrations. *Spectrochim. Acta, Part A* **1972**, *28*, 2091−2101.
(45) Wolff, H.; Wolff, E. Hydrogen Bonding and Fermi Resonance of N-Propylamine. Comparison of the Results from IR and Raman Measurements. *Spectrochim. Acta, Part A* **1988**, *44*, 1273−1275.
(46) Smith, D. F., Jr.; Overend, J. Anharmonic Force Constants of Water. *Spectrochim. Acta, Part A* **1972**, *28*, 471−483.
(47) Worley, J. D.; Klotz, I. M. Near Infrared Spectra of H_2O—D_2O Solutions. *J. Chem. Phys.* **1966**, *45*, 2868.
(48) Auer, B.; Kumar, R.; Schmidt, J. R.; Skinner, J. L. Hydrogen Bonding and Raman, IR, and 2D-IR Spectroscopy of Dilute HOD in Liquid D_2O. *Proc. Natl. Acad. Sci. U.S.A.* **2007**, *104*, 14215−14220.
(49) Bakker, H. J.; Nienhuys, H.-K.; Gallot, G.; Lascoux, N.; Gale, G. M.; Leicknam, J.-C.; Bratos, S. Transient Absorption of Vibrationally Excited Water. *J. Chem. Phys.* **2002**, *116*, 2592.
(50) Bakker, H. J.; Nienhuys, H.-K. Delocalization of Protons in Liquid Water. *Science (New York, N.Y.)* **2002**, *297*, 587−590.
(51) Laenen, R.; Rauscher, C.; Laubereau, A. Local Substructures of Water Studied by Transient Hole-Burning Spectroscopy in the Infrared: Dynamics and Temperature Dependence. *J. Phys. Chem. B* **1998**, *102*, 9304−9311.
(52) Roberts, S. T.; Ramasesha, K.; Tokmakoff, A. Structural Rearrangements in Water Viewed Through Two-Dimensional Infrared Spectroscopy. *Acc. Chem. Res.* **2009**, *42*, 1239−1249.
(53) Bakulin, A. A.; Pshenichnikov, M. S.; Bakker, H. J.; Petersen, C. Hydrophobic Molecules Slow Down the Hydrogen-Bond Dynamics of Water. *J. Phys. Chem. A* **2011**, *115*, 1821−9.
(54) Petersen, C.; Bakulin, A. A.; Pavelyev, V. G.; Pshenichnikov, M. S.; Bakker, H. J. Femtosecond Midinfrared Study of Aggregation Behavior in Aqueous Solutions of Amphiphilic Molecules. *J. Chem. Phys.* **2010**, *133*, 164514.
(55) Golonzka, O.; Tokmakoff, A. Polarization-Selective Third-Order Spectroscopy of Coupled Vibronic States. *J. Chem. Phys.* **2001**, *115*, 297.
(56) Fair, J. R.; Votava, O.; Nesbitt, D. J. OH Stretch Overtone Spectroscopy and Transition Dipole Alignment of HOD. *J. Chem. Phys.* **1998**, *108*, 72−80.
(57) Khoshtariya, D. E.; Dolidze, T. D.; Lindqvist-Reis, P.; Neubrand, A.; Van Eldik, R. Liquid Water (D_2O): A Dynamic Model Emerging from Near-Infrared DOD Stretching Overtone Studies. *J. Mol. Liq.* **2002**, *96*−*97*, 45−63.
(58) Lock, A. J.; Woutersen, S.; Bakker, H. J. Ultrafast Energy Equilibration in Hydrogen-Bonded Liquids. *J. Phys. Chem. A* **2001**, *105*, 1238−1243.
(59) Steinel, T.; Asbury, J. B.; Zheng, J.; Fayer, M. D. Watching Hydrogen Bonds Break: A Transient Absorption Study of Water. *J. Phys. Chem. A* **2004**, *108*, 10957−10964.
(60) Fecko, C. J.; Loparo, J. J.; Roberts, S. T.; Tokmakoff, A. Local Hydrogen Bonding Dynamics and Collective Reorganization in Water: Ultrafast Infrared Spectroscopy of HOD/D_2O. *J. Chem. Phys.* **2005**, *122*, 54506.
(61) Loparo, J.; Fecko, C.; Eaves, J.; Roberts, S.; Tokmakoff, A. Reorientational and Configurational Fluctuations in Water Observed on Molecular Length Scales. *Phys. Rev. B: Condens. Matter Mater. Phys.* **2004**, *70*, 180201.
(62) Gale, G. M.; Gallot, G.; Lascoux, N. Frequency-Dependent Vibrational Population Relaxation Time of the OH Stretching Mode in Liquid Water. *Chem. Phys. Lett.* **1999**, *311*, 123−125.
(63) Knop, S.; Jansen, T. L. C.; Lindner, J.; Vöhringer, P. On the Nature of OH-Stretching Vibrations in Hydrogen-Bonded Chains: Pump Frequency Dependent Vibrational Lifetime. *Phys. Chem. Chem. Phys.* **2011**, *13*, 4641−4650.
(64) Perakis, F.; Widmer, S.; Hamm, P. Two-dimensional Infrared Spectroscopy of Isotope-Diluted Ice Ih. *J. Chem. Phys.* **2011**, *13*, 204505.

NOTE ADDED IN PROOF

A recent 2DIR study of HOD/D_2O ice Ih[64] described non-adiabatic vibrational effects that may lead to induced absorptions in the 1500−3000 cm^{-1} spectral region. Calculations based on the Lippincott-Schroeder potential, which treats only the O-H and hydrogen bond stretches but not the bend, indicated that induced absorptions between mixed modes may also contribute. This may further complicate the description of vibrational modes and relaxation in the liquid.

dx.doi.org/10.1021/jp4034613 | J. Phys. Chem. B XXXX, XXX, XXX−XXX